

# Bright Variable Stars in NGC 6819 - An Open Cluster in the *Kepler Field*

Antonio Talamantes, Eric L. Sandquist

*San Diego State University, Department of Astronomy, San Diego, CA 92182*

atalaman@pleiades.sdsu.edu, erics@mintaka.sdsu.edu

James L. Clem

*Department of Physics & Astronomy, Louisiana State University, Baton Rouge, LA  
70803-4001*

jclem@phys.lsu.edu

Russell M. Robb, David D. Balam

*Department of Physics and Astronomy, University of Victoria, Victoria, BC, Canada,  
V8W 3P6*

robb@uvic.ca, cosmos@uvic.ca

Matthew Shetrone

*University of Texas, McDonald Observatory, HC75 Box 1337-L Fort Davis, TX, 79734*

shetrone@astro.as.utexas.edu

## ABSTRACT

We describe a variability study of the moderately old open cluster NGC 6819. We have detected 4 new detached eclipsing binaries near the cluster turnoff (one of which may be in a triple system). Several of these systems should be able to provide mass and radius information, and can therefore constrain the age of the cluster. We have also newly detected one possible detached binary member about 3.5 magnitudes below the turnoff. One EW-type binary (probably not a cluster member) shows unusually strong night-to-night light curve variations in sets of observations separated by 8 years.

According to the best current information, the three brightest variables we detected (2 of them new) are cluster members, making them blue stragglers. One is a  $\delta$  Scu pulsating variable, one is a close but detached binary, and the

third contains a detached short period binary that shows total eclipses. In each case, however, there is evidence hinting that the system may have been produced through the interaction of more than two stars.

*Subject headings:* binaries: eclipsing — open clusters and associations: individual (NGC 6819) — blue stragglers

## 1. Introduction

Star clusters have long been used as laboratories for testing our understanding of the physics that goes into computing models of stars. Most commonly, the brightnesses and colors of the stellar population have been compared with isochrones to check our understanding of how stars of nearly the same age and chemical composition evolve. Unfortunately, observational and theoretical issues prevent highly accurate measurements of desirable quantities like age. For example, convection and color- $T_{\text{eff}}$  relations present notorious problems in modeling the light emitted by stellar populations. Degeneracies in distance, interstellar reddening, chemical composition greatly complicate efforts to measure ages as well (Southworth et al. 2004, e.g.).

The different methods of deriving information about the stars in a population can magnify each other. The analysis of eclipsing binary stars can provide accurate mass and radius information on a subset of the stars, and when used in conjunction with colors and brightnesses, this can help to “pin down” theoretical isochrones at a number of locations. This immensely increases the constricting power of the observations. Asteroseismology can provide accurate mean densities for individual stars and holds promise of revealing details of their internal structure. But again, when these observation can be used with color-magnitude diagram information the power of the tests are magnified.

Star clusters in the field of the *Kepler* satellite promise to become important laboratories for stellar astronomy because of the range of observations that can be brought to bear to test theoretical models. Asteroseismological oscillations have already been detected in giant stars in the cluster NGC 6819 (Stello et al. 2010), and efforts are on to detect them among fainter stars. This paper is the start of our attempt to identify detached eclipsing binary stars in this same cluster. *Kepler* will provide light curves of unprecedented accuracy that will greatly improve the precision of radius measurements for stars in the cluster, but to make full use of the binary systems, we also need temperature information that will come from observations in narrower wavelength bands. In turn, masses for turnoff stars will help directly constrain the low-mass end of the white dwarf initial-final mass relation (Kalirai et al. 2001;

Williams et al. 2009, e.g.), which in turn impacts chemical enrichment and white dwarf cooling studies.

NGC 6819 is a moderately old cluster ( $\sim 2.5$  Gyr; Rosvick & Vandenberg 1998; Kalirai et al. 2001) with near-solar or slightly super-solar metallicity ( $[\text{Fe}/\text{H}] = +0.09 \pm 0.03$ ; Bragaglia et al. 2001). Variability studies have been presented previously for NGC 6819 by Kaluzny & Shara (1988), Street et al. (2002), and Street et al. (2005). The wider surveys of Hartman et al. (2004) and Pigulski et al. (2009) also covered large portions of the *Kepler* field as part of the Hungarian-made Automated Telescope network (HATnet) project and the All-Sky Automated Survey (ASAS), respectively. Both the HATnet and ASAS surveys had low spatial resolution ( $14''$  and  $15''$  per pixel) and were relatively shallow, so there is no overlap with the variables we discuss below. Kaluzny & Shara (1988) were searching for short period contact binaries in the cluster, and their observing program only involved two nights. Even so they identified three possible variables, two of which we have confirmed. (The third, which corresponds to star A81, was not seen to vary in our datasets.) In a series of papers, Street et al. identified a large number of variables in and near the cluster as a byproduct of a planet search. Their exposures resulted in saturation for stars with  $V \lesssim 16.5$ , which is fainter than the cluster turnoff. There was therefore a distinct possibility that undetected detached eclipsing variables were present in the cluster.

While characterization of the eclipsing binaries is our primary goal, accurate and precise stellar photometry needs to be of complementary quality. Auner (1974) presented the first wide field photographic photometry of NGC 6819, while the primary CCD photometry has been published by Rosvick & Vandenberg (1998) and Kalirai et al. (2001). The photometry in this study covers a slightly larger field and goes slightly fainter than that of Rosvick & Vandenberg (1998). By contrast, Kalirai et al.’s study covered a much wider field and went deep enough to identify the cluster’s white dwarf sequence.

## 2. Observations and Data Reduction

NGC 6819 was observed using two different telescopes. Some of us (J.L.C., R.M.R, D.D.B) observed the cluster for 10 consecutive nights using the 1.8 meter Plaskett Telescope at Dominion Astrophysical Observatory (hereafter, DAO) between July 5-15, 2001 (although weather compromised most of the night of July 7). These images were taken using a Cousins  $R$  filter (hereafter  $R_C$ ) and lasted for a total of 180 s each. The field of view, spanning a

---

<sup>0</sup>Identification numbers in this paper that start with “A” come from the photometric study by Auner (1974).

total area of  $9'2 \times 9'2$ . A  $1024 \times 1024$  CCD was used, and pixels were binned  $2 \times 2$ , for a final  $1''1$  per pixel. 16 nights of data were taken at the Mount Laguna Observatory (hereafter, MLO) 1 m telescope (by A.T. and E.L.S.) covering an area approximately  $13'5 \times 13'5$ , for a scale of about  $0''4$  per pixel. and are listed in Table 1. For eleven of the nights the exposures were taken using a  $V$  filter and typically lasted 90 s each. The remaining six nights of observations used a Kron  $R$  filter (hereafter  $R_K$ , which has a passband similar to the combination of Cousins  $R$  and  $I$ ) and again each exposure was typically 90 s. Two additional nights of observations were taken at MLO for the purpose of calibrating the photometry to the standard system. For both the DAO and MLO datasets, the seeing typically produced a FWHM of stellar images around  $2 - 2.5$  arcsec. Image reduction (overscan subtraction, bias subtraction, and flat field correction) was done using standard tools in IRAF<sup>1</sup>.

Differential photometry was undertaken using the image subtraction package ISIS (Alard 2000). ISIS is commonly used in variability studies today, thanks to its ability to detect variability at near the Poisson noise limit. Our image sets in  $V$ ,  $R_C$ , and  $R_K$  filters were interpolated to a common image coordinate system (separately for the DAO and MLO datasets), and then processed separately by filter. This involved producing a reference image from approximately 20 images with the best seeing; subtracting each interpolated image from the reference image once the reference was transformed to the seeing of the interpolated image (and a constant flux scaling is enforced); stacking the subtracted images to identify stars whose detected flux had changed; and taking photometric measurements of the subtracted image. While ISIS has the capability of breaking images into subimages and analyzing the point-spread function separately on each subimage, we found that using whole images produced better results for our datasets.

Several routines of the ISIS code do not function optimally, however. The ISIS code uses a bicubic spline to interpolate each image to the coordinate system set by an astrometric reference image. Bicubic splines are subject to spurious oscillations near sharp features though, so we replaced the bicubic spline with an Akima spline. This reduced noise that had been introduced by saturated stars and diffraction spikes, but also improved the interpolation of the images of bright stars on images with good seeing.

The output of ISIS is a difference flux measured on the subtracted images. To convert these difference fluxes into magnitudes, the star's flux must be measured on the reference frame. For crowded star fields, this should ideally be done using a technique like profile fitting

---

<sup>1</sup>IRAF (Image Reduction and Analysis Facility) is distributed by the National Optical Astronomy Observatories, which are operated by the Association of Universities for Research in Astronomy, Inc., under contract with the National Science Foundation.

that is capable of accurate photometry in the limit of strongly overlapping star images. An important issue is that a flux derived in that way is not guaranteed to be on the same scale as the ISIS difference flux (Hartman et al. 2004), and if it is not, this will directly affect the amplitude of derived light curves. For our datasets, we found that a reference flux derived from ISIS’ own photometry routine was a reliable choice. We are principally interested in ensuring that our *differential* photometry is accurate because this affects the reliability of stellar sizes computed from light curve analysis. To this end, we subtracted our aperture photometry results from ISIS photometry point-by-point for a selection of eclipsing binary stars that were not affected by blending issues. When done, it was impossible to distinguish between points in or out of eclipses.

ISIS’ algorithm is a modified aperture photometry routine that employs the reference image point-spread function (PSF) for weighting purposes. The reference PSF is first transformed to the seeing of the image under consideration. Only the portion within an aperture of `radphot` pixels is used, but it is normalized to a larger aperture of `rad_aper` pixels. The pixel values in the subtracted image are weighted by this transformed PSF. For the MLO datasets, we used `radphot` = 4 pix and `rad_aper` = 10 pixels. For the DAO images (which had pixels with larger area on the sky), we used `radphot` = 2 pix and `rad_aper` = 7. The photometry routine requires coordinate lists for the stars to be measured — both centroid and pixel with maximum counts. As written, ISIS uses the pixel with maximum counts as the center of the apertures. It should be noted that the ISIS starts its pixel coordinate system at  $x = y = 0$ , unlike many astronomical software packages, and this should be accounted for if producing a coordinate list outside of ISIS’ routines.

Finder charts for the detected variables are shown in Fig. 1.

## 2.1. Photometric Calibration

We took calibration images under photometric conditions on the night of 25 October 2008. We observed the standard fields PG0231+051, SA 92, SA95, SA 98, and NGC 6940, and used standard values taken from Stetson (2000, retrieved August 2009). The standard fields were observed between 3 and 10 times per filter in *BVI* at airmasses that ranged from 1.034 to 1.998. All together this resulted in more than 4000 standard star observations per filter covering a color range  $-0.5 \lesssim (B - I) \lesssim 5$ .

We derived aperture photometry from all frames using DAOPHOT, and made curve of growth corrections using the program DAOGROW. The observations were transformed to

the standard system using the following equations:

$$b = B + a_0 + a_1(B - I) + a_2X$$

$$v = V + b_0 + b_1(B - I) + b_2X$$

$$i = I + c_0 + c_1(B - I) + c_2X$$

where  $b$ ,  $v$ , and  $i$  are instrumental magnitudes,  $B$ ,  $V$ , and  $I$  are standard-system magnitudes,  $X$  is airmass, and  $a_i$ ,  $b_i$ , and  $c_i$  are coefficients determined from least-squares fits. For the color coefficients, we found  $a_1 = -0.0208 \pm 0.0018$ ,  $b_1 = 0.0367 \pm 0.0007$ , and  $c_1 = -0.0066 \pm 0.0006$ . The extinction coefficients were  $a_2 = 0.233 \pm 0.004$ ,  $b_2 = 0.129 \pm 0.005$ , and  $c_2 = 0.064 \pm 0.007$ . Fig. 2 shows the residuals of the comparison of our standardized observations and the Stetson values.

Clusters to be calibrated were observed with a range of exposures times on the same night. For NGC 6819, there were 8 observations in  $B$  ( $1 \times 30$  s,  $2 \times 60$  s,  $2 \times 120$  s,  $2 \times 180$  s, and  $1 \times 300$  s), 9 observations in  $V$  ( $2 \times 10$  s,  $2 \times 60$  s,  $4 \times 120$  s, and  $1 \times 300$  s), and 11 observations in  $I$  ( $4 \times 10$  s,  $1 \times 60$  s,  $5 \times 120$  s, and  $1 \times 300$  s).

Figure 3 shows a comparison of our photometry with that of Rosvick & Vandenberg (1998), as downloaded from the WEBDA database. It should be noted that Rosvick & Vandenberg did not present the details of the  $I_C$  observations or reduction in their article, Overall there is no sign of color-dependent residuals and there is very good agreement in zeropoints, with the most noticeable difference being a relatively large zeropoint difference in  $I_C$ . The color-magnitude diagram for our field is shown in Fig. 4.

## 2.2. Spectra

Our spectra were obtained at the Hobby-Eberly Telescope (HET) with the High Resolution Spectrograph (HRS, Tull 1998) as part of normal queue scheduled observing (Shetrone et al. 2007). HRS was configured to HRS\_30k\_central\_316g5936\_2as\_0sky\_ISO\_GC0\_2x3 or HRS\_30k\_central\_600g5 to achieve R=30,000 spectra covering 4100Å to 7800Å or 4825Å to 6750Å respectively. Exposure times ranged from 600 seconds to 1200 seconds. The signal-to-noise was typically 25 per resolution element at 5800 Å.

The spectra were reduced with IRAF ECHELLE scripts. The standard IRAF scripts for overscan removal, bias subtraction, flat fielding and scattered light removal were employed. For the HRS flat field we masked out the Li I, H I and Na D regions because the HET HRS flat field lamp suffered from faint emission lines. The spectra were combined into a single

long spectrum for the blue and red chips. Radial velocities were determined from cross-correlation using the IRAF task `fxcor` using a solar spectrum as template. The heliocentric correction was made using the IRAF task `rvcorrect`.

### 3. Results

#### 3.1. Pulsating Star A20pe

This star<sup>2</sup> has identification number 107 in the proper motion study of Sanders (1972), which gives it a 90% probability of membership. It is as bright in  $V$  as stars in the red clump for the cluster, but is bluer than the cluster turnoff. A20pe is therefore a likely cluster blue straggler.

The star has low-amplitude short period variation that identifies it as a  $\delta$  Scu pulsating variable. As such, it should be within the instability strip. We transformed the theoretical instability strip boundaries of Pamyatnykh (2000) to the observational plane using color- $T_{\text{eff}}$  relations from Vandenberg & Clem (2003), and  $E(B - V) = 0.10$  and  $(m - M)_V = 12.30$  (Kalirai et al. 2001). Based on this, the star appears to be too blue and/or bright. It is possible that the star could have a companion that is putting it out of the strip — a direct analog to this idea exists in the blue straggler EX Cnc in M67, which is an eccentric spectroscopic binary of 4.2 d period containing a  $\delta$  Scuti variable (Milone & Latham 1992). However, in this case, the companion star would have to be *hotter* and more massive than the  $\delta$  Scu star, implying that there would be two stars in a binary that would be identified as blue stragglers on their own. Radial velocities would be helpful in verifying the star's membership in the cluster, and if a member, helping to identify its formation mechanism.

#### 3.2. Contact or Near-Contact Binaries

Phased light curves for some of the short-period eclipsing binaries are shown in Fig. 6. Where possible, the photometry presented in Table 2 has been corrected to system maximum values. Most of these systems were previously identified by Street et al. (2002), and so we focus here on new systems and unusual properties of the known systems that have not been

---

<sup>2</sup>This is photoelectric standard 20 in Auner (1974), not part of his photographic photometry list. The identifications of this star seem to be confused in the WEBDA database. This is star 36 in the photometry of Rosvick & Vandenberg (1998), but that star is incorrectly identified with star 168 in the Sanders (1972) proper motion study.

discussed before.

Before discussing those, we attempted to estimate likelihood of membership using the color-luminosity relationship for W UMa variable stars from Rucinski & Duerbeck (1997):

$$M_V = -4.44 \log P + 3.02(B - V)_0 + 0.12$$

and then comparing the implied distance modulus to the one derived from isochrone fitting.  $(B - V)_0$  is the dereddened color of the system at maximum brightness. Kalirai et al. (2001) derived a distance modulus  $(m - M)_V = 12.30 \pm 0.12$  and assumed a reddening  $E(B - V) = 0.10$ . Given the uncertainty in the distance modulus and the observed scatter of 0.22 mag in the Rucinski & Duerbeck (1997) relationship, V2396 Cyg [ $(m - M)_V = 12.26$ ], V2388 Cyg (12.53) are probable cluster members, while A355 (11.47) and V2389 Cyg (14.39) are not. We discuss the special case WOCS 013016 immediately below.

**WOCS 013016:** This is a new detection because it was too bright for the variability surveys by Street et al. (2002, 2005) and was outside the field studied by Kaluzny & Shara (1988). The  $V$  photometry presented in Table 2 has been corrected to maximum system brightness, but the colors are somewhat less accurate — our calibration observations occurred near, but not at maximum light.

The system has identification number 46 in the proper motion study of Sanders (1972), which gives it a 80% probability of membership. If we apply the Rucinski & Duerbeck (1997) period-luminosity-color (PLC) relationship here, we calculate  $(m - M)_V = 12.38$ , in very good agreement with the cluster distance modulus. However, WOCS 013016 has a period that is significantly longer than the probable cluster EW systems that we detected, and its light curve more closely resembles those of EB systems. Rucinski & Duerbeck (1997) discuss the application of their period-luminosity-color (PLC) relationship to EW systems that appear to be in poor thermal contact (in other words, having eclipses of significantly different depths, implying significant differences in the surface temperatures of the components). They indicate that the PLC relationship should produce luminosity estimates that are too high. As long as the biases are not too large ( $\lesssim 0.3$  mag), the distance modulus for WOCS 013016 supports its membership in the cluster.

If it is a member, then it should be identified as a blue straggler that is probably in the process of coalescing. To be as blue as it is currently, there must have been an earlier merger or significant mass transfer to have produced the more massive component of the binary.

**A355 (WOCS 052004):** This variable is brighter than the saturation limit for images



taken by Street et al. (2002), but was detected earlier by Kaluzny & Shara (1988).<sup>3</sup> This binary system is probably in contact, but it shows *unusually severe* distortions to its light curve, as seen in Fig. 7. Similar behavior was seen also in  $V$  and  $R_K$  filter bands with a different telescope/camera set-up years later, so this behavior is very likely to be real and ongoing. For example, in several cases in the figure (and on the nights HJD 2454697 to 2454699), the photometric maximum is found as much as 0.1 cycle away from the expected position, and it shifts significantly from night to night. In other cases (HJDs 2452103 and 2452105 in the figure, as well as HJDs 2454624 and 2454669), one of the photometric maximums was almost completely truncated, to the point of making the system superficially resemble a detached eclipsing binary of nearly spherical stars. Before and after night 2452103, the system showed some of its deepest eclipses and showed variations identifying it as an EW system with gravitationally distorted stars of nearly equal temperature. In nearly all cases where we can compare phases 0.5 apart on the same night, the light curves imply the system is nearly point symmetric about the center of the orbits, but not symmetric about the line connecting the star centers. This type of variation is difficult to understand in terms of spots in part because of the symmetry and in part because of the short timescales.

The distortions of the light curve made it difficult to derive a period, but the value given in Table 2 does a good job of align the eclipses in phase. While we attempted to correct the system photometry to maximum light, we do not have light curve information during the calibration observations, so that we are not full able to judge what kind of variations might have been occurring. While the distortions of the light curve are interesting, because the object does not appear to be a cluster member, we do not discuss it further here.

**V2389 Cyg:** Although this system does not appear to be a cluster member, it does have total eclipses, as noted by Street et al. (2002). We note additionally that we detected a sudden change in the depth of one eclipse from one night to the next (see Fig. 8). On the nights of HJD 2454697 through 2454699, we observed both eclipses on individual nights, and while they were of equal depth on the first two nights, on the third night one of the eclipses had increased in brightness by approximately 0.1 mag. We only observed two later eclipses in the same filter band, but both were at the brighter level.

**V2394 Cyg:** According to the PLC analysis, this binary appears to be a cluster member. The system shows short timescale ( $\sim 0.14$  d) variations reminiscent of a contact binary, and long timescale variations in overall brightness level (see Fig. 9). Both types of varia-

---

<sup>3</sup>This star is labeled as “V2” in the finder chart of Kaluzny & Shara (1988), but their tabulated photometry and the position of V2 in their CMD is not consistent with our photometry. We believe that “V1” in their table and CMD corresponds to this variable.

tions make it difficult to derive an accurate period, but it is clear that it is close to that of Street et al. (2002).

### 3.3. Detached Eclipsing Binaries (DEBs)

Cluster members that are DEBs were one of the main goals of this study because of their ability to provide masses and radii. Of the newly detected DEBs, the most interesting are A494 (a possible blue straggler), A259, A536, and A665 (near the cluster turnoff), and ID 1602 (faint main sequence). The stars below are ordered by brightness.

**A494 (WOCS 007006):** Although this system was discovered to be variable by Kaluzny & Shara (1988), they were unable to fully characterize the system due to their small number of observations. For the first time, we detect clear evidence of total eclipses in this short period binary, with only a small amount of variation outside of eclipse (see Fig. 10). There appears to be a small difference in eclipse depths with this period, although we see some variation in depth that may be an indication of spot activity. (Note that A494 was close to saturating pixels in the DAO images, so the variations there should not be taken as necessarily representing the stellar variability.) As a result, there is some possibility that the true period is twice what we quote in Table 2. The shallowness of the total eclipses ( $\sim 0.14$  mag) is a strong indication that there is a third star present that contributes most of the system’s light. We have two spectra taken the HET (see Table 3) that only show one clearly detectable component.

The system has identification number 59 in the proper motion study of Sanders (1972), who gave it a 57% probability of membership. The radial velocities of the brightest star at the two epochs are significantly different from each other and one is significantly different from the cluster mean ( $2.34 \pm 0.05$  km s<sup>-1</sup> with a dispersion  $\sigma = 1.02 \pm 0.02$  km s<sup>-1</sup>; Hole et al. 2009), indicating that it may be showing a reflex motion in response to the gravity of the eclipsing binary. We can estimate that the rotational velocity of the brightest star is  $60 \pm 10$  km s<sup>-1</sup>. If it is a cluster member, it is likely that the third component is a blue straggler star in its own right, and the close binary contains relatively low-mass main sequence stars. Using the eclipse depths as guides, we find that we can reproduce the system photometry with two cluster main sequence stars with  $16.1 \lesssim V \lesssim 16.4$ , which would in turn result in a third star ( $V \approx 14.4$ ) falling near an extension of the cluster main sequence. That would make A494 an example of a blue straggler system that must have formed from a binary-binary star interaction. The straggler S1082 in the open cluster M67 presents a more extreme example in which 5 or more stars may have been involved in producing the three stars that are observed today (van den Berg et al. 2001; Sandquist et al. 2003). Another

example is the star 7782 in the older cluster NGC 188, which appears to involve two blue stragglers in a binary system (Geller et al. 2009). If the radial velocities of the stars in the eclipsing binary could be measured, it might be possible to determine the masses of all three stars.

**A259 (WOCS 040007):** There was an eclipse during some of our calibration observations, although we had others on the same night that allowed us to calculate reliable system values. Spectra show two components (A. Geller & R. Mathieu, private communication). The phased light curves are shown in Fig. 11. The observations in  $R_K$  reveal that there is a short period (about 45 min) of totality in both eclipses. Based on all of this information, this system is an excellent candidate for deriving mass and radius information for the component stars.

**A536 (WOCS 022003):** The interval between two eclipses of different depth observed in 2001 was about 2.12 d. However, the remainder of our observations contain only partial coverage of several eclipses and were separated by large time intervals. Radial velocity information (A. Geller & R. Mathieu, private communication) allowed us to identify a period of 4.30103 d, which in turn indicates that the eccentricity is near zero. (Phased light curves are shown in Fig. 12.) The radial velocities also indicate that the more massive star is farther from us during the deeper eclipse in  $R_C$ , as expected if both stars are on the main sequence.

A536 shows three components in spectra (A. Geller & R. Mathieu, private communication; Table 3). Because the brighter stars are part of the eclipsing binary, it should be possible to derive mass and radius information for them. The third component may explain other peculiarities of the photometric observations — most notably that there are deep eclipses observed in  $R_K$  at the same phase when a clear secondary eclipse was observed in  $R_C$ . We emphasize that radial velocities clearly rule out other possible periods. There is a star about  $1''.6$  south of A536 that was not resolved in  $R_C$  that is probably influencing the measured eclipse depths. This star appears to be WOCS 34003, which has  $V = 15.66$  and  $B - V = 0.62$ . Our images in  $R_K$  have the best spatial resolution, which probably results in less dilution of the binary’s light.

The nearby star is also a possible contaminant in the spectra used for radial velocities because in poor seeing conditions its light could enter the fiber optic cables used in the spectrograph. (The cables have sky widths of  $2''$  for the HET spectra and  $3''$  for the Geller & Mathieu spectra.) The third component in spectra appears near the cluster mean in agreement with this idea. If true, this system could still provide a good age constraint for the cluster.

This object is an interesting test of how well image subtraction photometry can do in deriving precise light curves in a moderately crowded stellar environment. In a high-precision light curve from the *Kepler* mission, these stars will undoubtedly be blended due to the nearly 4" pixels. We are continuing work on this system with the aim of doing a full analysis of the eclipsing binary. At worst it should be possible to treat the nearby star as a “third light” contributor that dilutes the binary’s light, but with higher resolution observations the true eclipse depths should be measurable.

**A665 (WOCS 024009):** We have not yet been able to identify a period for the system due to a combination of partial coverage of eclipses and no indication yet that the eclipses have different depths. Fig. 13 shows our detections of parts of eclipses. High-precision *Kepler* light curves should be able to identify differences in eclipse depths and enable a period determination. In any case, this is likely to be the eclipsing binary with the longest period detected in this survey. Spectra indicate that the system has three components (A. Geller & R. Mathieu, private communication). There is no indication of a resolvable blended star, so this system may be a triple. At least one of the brighter stars in the group is in the eclipsing binary, so it should be possible to derive mass and radius information.

**A824 (WOCS 059010):** This system shows eclipses of moderate ( $\sim 0.15$  mag) depth (see Fig. 14). Parts of eclipses were detected on 8 of the 10 nights of the DAO photometry observations, implying a period of a day or less. The small size of the out-of-eclipse variation (as much as 0.02 mag) indicates that the correct period is probably the longest possible acceptable period. This led to the identified period of approximately 0.787 d. Because the eclipses are of similar depth and because there are out-of-eclipse variations (probably due to magnetic activity), it is hard to definitively identify a primary and secondary eclipse.

In our best seeing images, this star appears to be a marginally resolvable blend, with a separation of about 1".2 along an axis ESE to WNW. The blend probably affects the depths of the eclipses in all filter bands, but especially in the lower-resolution  $R_C$  from DAO. Spectra have only detected a cluster non-member with constant radial velocity (Hole et al. 2009). The detected eclipsing binary has a very short period for a binary that shows little out-of-eclipse variation, and so this reinforces the idea that the eclipsing binary is composed of small faint main sequence stars. Because of the possibility the binary could be a cluster member, we are studying this system further, although the much brighter nonmember star will make spectroscopic analysis more difficult.

**V2381 Cyg:** A primary eclipse occurred on the night of our calibration observations, affecting all of our measurements. We were able to correct the  $V$  measurements to out-of-eclipse values using the differential photometry, but this is not yet possible with the  $B$  and  $I$  measurements. The quoted  $B - V$  color in Table 2 comes from Street et al. (2002), and

puts the system well to the blue of the main sequence. CMDs using instrumental magnitudes from nights without eclipses confirm that the system is bluer than the cluster main sequence. The implication is that the system is not a cluster member.

**ID 1602 (2MASS 19410280+4007116):** The photometry for this system places it between the single-star main sequence and the equal-mass binary sequence. We detected three deep ( $\sim 0.8$  mag) partial eclipses in  $V$ , one shallower ( $\sim 0.6$  mag) eclipse in  $R_K$ , and part of four eclipses in  $R_C$ . Three eclipses observed in  $R_C$  were each separated by a little over two days, and the middle one appears to be a shallower secondary eclipse. We believe a period of 4.1108 d is most likely, and the data is phased to this period in Fig. 15.

#### 4. Conclusions

One of the primary discoveries in this study was three variable blue stragglers which each present evidence of formation through binary-moderated dynamical interactions. These stars exist in NGC 6819 alongside four additional blue straggler systems that show velocity variability (Hole et al. 2009) indicative of binarity, although the history of these systems cannot yet be reconstructed. These results emphasize how photometric and spectroscopic studies of blue stragglers are complementary — photometric studies tend to be biased toward the discovery of short-period binary systems, while spectroscopy is essentially the only way of discovering populations of long-period binaries (Geller et al. 2009, e.g.). However, together the photometric and radial velocity variables only account for about 50% of the blue straggler population in this cluster. Spectroscopic abundance studies (Shetrone & Sandquist 2000; Ferraro et al. 2006, e.g.) provide another avenue for delving into blue straggler formation histories even for single stars.

More importantly though, we have uncovered four detached eclipsing binary systems near the cluster turnoff of NGC 6819. Three of the systems are very likely to be cluster members, and the membership of the fourth is still to be determined. Because of the selection bias against photometrically detecting long period eclipsing binary systems, there is a fair chance that others are present (Rucinski et al. 1996, e.g.). The *Kepler* satellite provides an ideal means of detecting additional systems in NGC 6819. If all of these systems are fully analyzed to derive masses and radii for the eclipsing components, they will densely constrain theoretical stellar models near the turnoff.

We thank A. Geller and R. Mathieu for valuable conversations on the spectra of some of the binaries, and K. Brogaard for comments on the manuscript. We would like to thank the Director of Mount Laguna Observatory (P. Etzel) for generous allocations of observing

time. Infrastructure support for the observatory was generously provided by the National Science Foundation through the Program for Research and Education using Small Telescopes (PREST) under grant AST 05-19686. We would also like to thank A. Bostroem, C. Gabler, and J. B. Leep for assisting with the photometric calibration observations.

This work has been funded through grant AST 09-08536 from the National Science Foundation to E.L.S. A.T. gratefully acknowledges the support of the NSF through grant AST 04-53609 as part of the CSUURE Research Experiences for Undergraduates (REU) program at San Diego State University.

The Hobby-Eberly Telescope (HET) is a joint project of the University of Texas at Austin, the Pennsylvania State University, Stanford University, Ludwig-Maximilians-Universität München, and Georg-August-Universität Göttingen. The HET is named in honor of its principal benefactors, William P. Hobby and Robert E. Eberly. This research made use of the SIMBAD database, operated at CDS, Strasbourg, France, and the WEBDA database, operated at the Institute for Astronomy of the University of Vienna.

## REFERENCES

- Alard, C. 2000, *A&AS*, 144, 363
- Auner, G. 1974, *A&AS*, 13, 143
- Bragaglia, A., et al. 2001, *AJ*, 121, 327
- Ferraro, F. R., et al. 2006, *ApJ*, 647, L53
- Geller, A. M., Mathieu, R. D., Harris, H. C., & McClure, R. D. 2009, *AJ*, 137, 3743
- Hartman, J. D., Bakos, G., Stanek, K. Z., & Noyes, R. W. 2004, *AJ*, 128, 1761
- Hole, K. T., Geller, A. M., Mathieu, R. D., Platais, I., Meibom, S., & Latham, D. W. 2009, *AJ*, 138, 159
- Kalirai, J. S., et al. 2001, *AJ*, 122, 266
- Kaluzny, J., & Shara, M. M. 1988, *AJ*, 95, 785
- Milone, A. A. E., & Latham, D. W. 1992, *Evolutionary Processes in Interacting Binary Stars*, 151, 475
- Pamyatnykh, A. A. 2000, *Delta Scuti and Related Stars*, 210, 215

- Pigulski, A., Pojmański, G., Pilecki, B., & Szczygiel, D. M. 2009, *AcA*, 59, 33
- Rosvick, J. M., & Vandenberg, D. A. 1998, *AJ*, 115, 1516
- Rucinski, S. M. & Duerbeck, H. W. 1997, *PASP*, 109, 1340
- Rucinski, S. M., Kaluzny, J., & Hilditch, R. W. 1996, *MNRAS*, 282, 705
- Samus, N. N., Durlevich, O. V., et al. 2009, *Vizie Online Data Catalog*, 1, 2025 (GCVS)
- Sanders, W. L. 1972, *A&A*, 19, 155
- Sandquist, E. L., Latham, D. W., Shetrone, M. D., & Milone, A. A. E. 2003, *AJ*, 125, 810
- Shetrone, M., et al. 2007, *PASP*, 119, 556
- Shetrone, M. D., & Sandquist, E. L. 2000, *AJ*, 120, 1913
- Southworth, J., Maxted, P. F. L., & Smalley, B. 2004, *MNRAS*, 349, 547
- Stello, D., et al. 2010, *ApJ*, 713, L182
- Stetson, P. B. 2000, *PASP*, 112, 925
- Street, R. A., et al. 2002, *MNRAS*, 330, 737
- Street, R. A., et al. 2005, *MNRAS*, 358, 795
- Tull, R. G. 1998, *Proc. SPIE*, 3355, 387
- VandenBerg, D. A., & Clem, J. L. 2003, *AJ*, 126, 778
- van den Berg, M., Orosz, J., Verbunt, F., & Stassun, K. 2001, *A&A*, 375, 375
- Williams, K. A., Bolte, M., & Koester, D. 2009, *ApJ*, 693, 355

Table 1. Photometry at Mount Laguna Observatory

Date	Filters	mJD Start <sup>a</sup>	<i>N</i>
Mar. 4, 2001	<i>V</i>	1973.994	53
Jun. 5, 2008	<i>V</i>	4623.715	137
Jun. 6, 2008	<i>V</i>	4624.714	134
Jun. 7, 2008	<i>V</i>	4625.715	96
Jul. 21, 2008	<i>V</i>	4669.659	168
Aug. 18, 2008	<i>R<sub>K</sub></i>	4697.649	246
Aug. 19, 2008	<i>R<sub>K</sub></i>	4698.649	231
Aug. 20, 2008	<i>R<sub>K</sub></i>	4699.645	218
Oct. 6, 2008	<i>VR<sub>K</sub></i>	4746.604	10,14
Oct. 25, 2008	<i>BVI<sub>C</sub></i>	4765.624	8,7,11
Mar. 30, 2009	<i>R<sub>K</sub></i>	4921.896	110
Jun. 9, 2009	<i>V</i>	4992.715	127
Jun. 10, 2009	<i>V</i>	4993.839	79
Jun. 11, 2009	<i>V</i>	4994.701	147
Sep. 6, 2009	<i>V</i>	5081.619	114
Sep. 10, 2009	<i>R<sub>K</sub></i>	5085.618	73
Oct. 21, 2009	<i>V</i>	5126.590	59
Nov. 15, 2009	<i>V</i>	5151.560	56

<sup>a</sup>mJD = HJD - 2450000.



Table 2. Variables Detected in the NGC 6819 Field

Identifications <sup>a</sup>		RA	DEC	$P$ (d)	$V$	$B-V$	$V-I$	Type	$\Delta V$	Min. mJD <sup>b</sup>	Notes
WOCS/GCVS	A74 KS88/S02										
007002	20pe	19:41:17.42	+40:11:03.6	0.155	12.80	0.21	0.28	$\delta$ Scu	0.09		blue straggler?
007006	494	V3	19:41:03.29	+40:10:52.8	0.932209	14.08	0.28	EA	0.16,0.13	5081.805	total eclipses, blue strag
013016			19:40:57.33	+40:04:55.7	0.666225	14.10	0.37	EB	0.55,0.22	5081.807	blue straggler
022003	536		19:41:12.07	+40:11:00.4	4.30103	14.93	0.61	EA	0.18	4698.655	phot. blend with nearby
059010	824		19:41:06.43	+40:07:48.2	0.787121	15.10	0.72	EA	0.15	4698.688	prob. blend with nearby
024009	665		19:40:57.85	+40:09:27.5		15.17	0.65	EA	$\sim 0.2$	2104.871	prob. triple
040007	259		19:41:33.94	+40:13:00.5	3.1851	15.65	0.71	EA	0.43	4698.730	
052004	355	V1/V2	19:41:25.87	+40:12:22.2	0.348687	15.71	0.79	EW	0.19	4697.727	
V2388	44	5834	19:41:10.33	+40:15:18.3	0.366025	16.53	0.74	EW	0.33	4697.705	
V2396		3856	19:41:28.58	+40:16:24.8	0.293151	17.11	0.88	EW	0.22	4697.746	
V2381		7916	19:40:44.83	+40:09:23.0	1.468	17.35	0.66	EA	1.3	4994.832	prob. nonmember
V2393		4448	19:41:22.61	+40:11:07.1	0.303209	17.37	0.97	EW	0.10	4697.724	
V2389		5660	19:41:11.73	+40:06:39.7	0.33847	18.04	0.58	EW	0.39	4697.870	prob. nonmember
V2394		4441	19:41:22.91	+40:14:39.5	0.2561	18.19	1.01	EW			
1602			19:41:02.80	+40:07:11.7	4.1108	19.00	1.24	EA	0.8	4994.74	

<sup>a</sup>WOCS: WIYN Open Cluster Survey; GCVS: General Catalogue of Variable Stars, Samus et al. (2009); A74: Auner (1974); KS88: Kaluzny & Shara (1988); (2002)

<sup>b</sup>mJD = HJD - 2450000.

Table 3. HET Radial Velocity Measurements

UT Date	mJD	$v_A$ (km s <sup>-1</sup> )	$\sigma_A$	$v_B$ (km s <sup>-1</sup> )	$\sigma_B$	$v_C$ (km s <sup>-1</sup> )	$\sigma_C$
A494:							
20091115	5150.56878	-39.5	8.9	223.8:	7.1		
20100602	5349.77955	-11.1	6.3				
A536:							
20091114	5149.56803	-64.3	1.0	80.3	2.6	-3.4	10.2:

<sup>a</sup>mJD = HJD - 2450000.

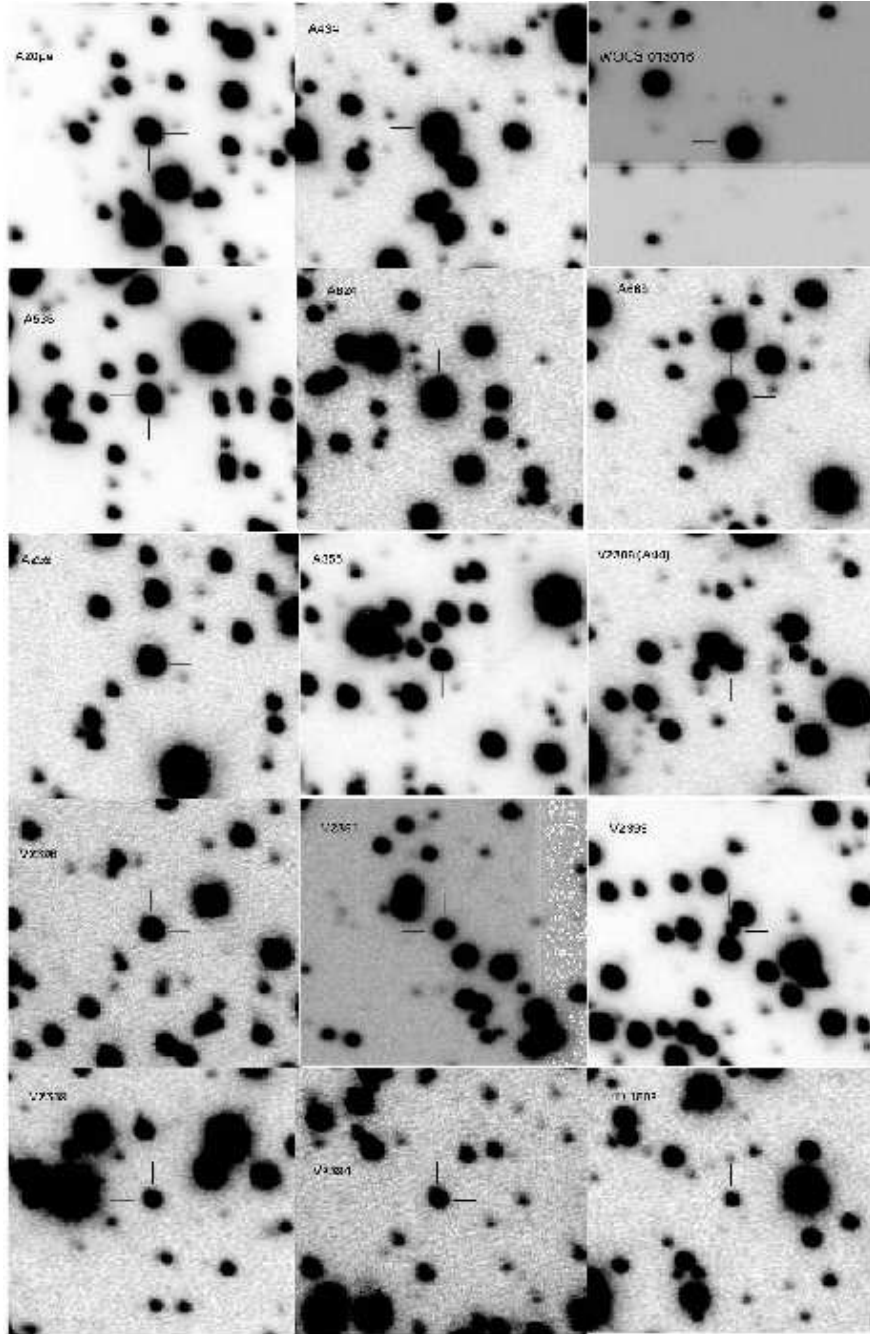


Fig. 1.— Finder charts in  $V$  band for the variables in NGC 6819 described in this paper. Individual squares are approximately  $1'$  across, and are oriented so north is at the top and east is to the left.

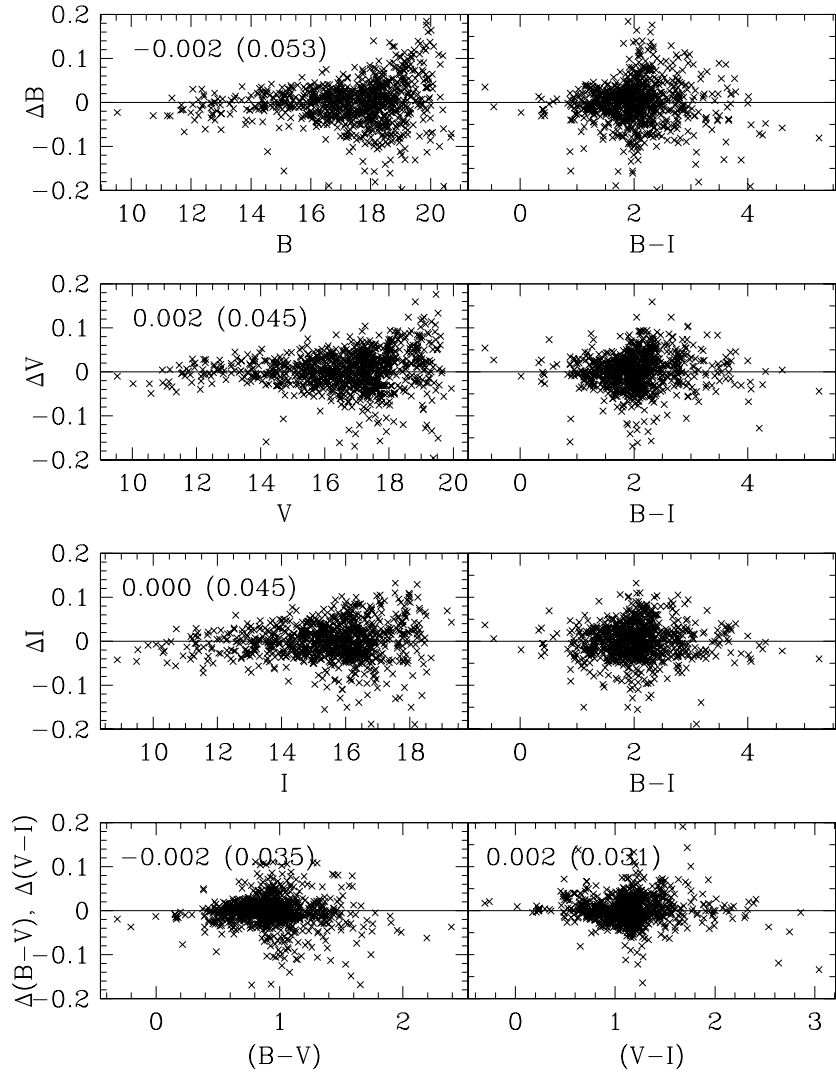


Fig. 2.— Residuals between our calibrated photometry of photometric standards and the standard magnitudes of Stetson 2000 (in the sense of this study minus Stetson’s).

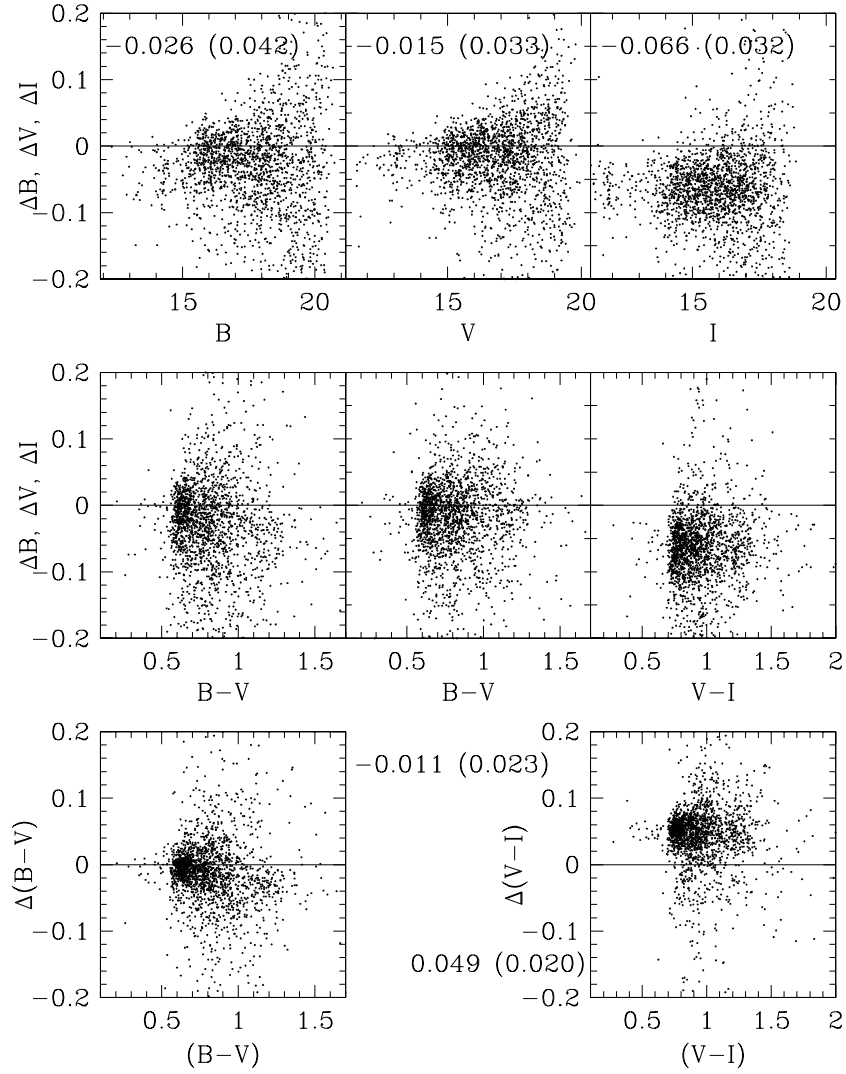


Fig. 3.— Residuals between our photometry of NGC 6819 and that of Rosvick & Vandenberg (1998), in the sense of this study minus theirs. The quoted numbers are the median residual and the semi-interquartile range.

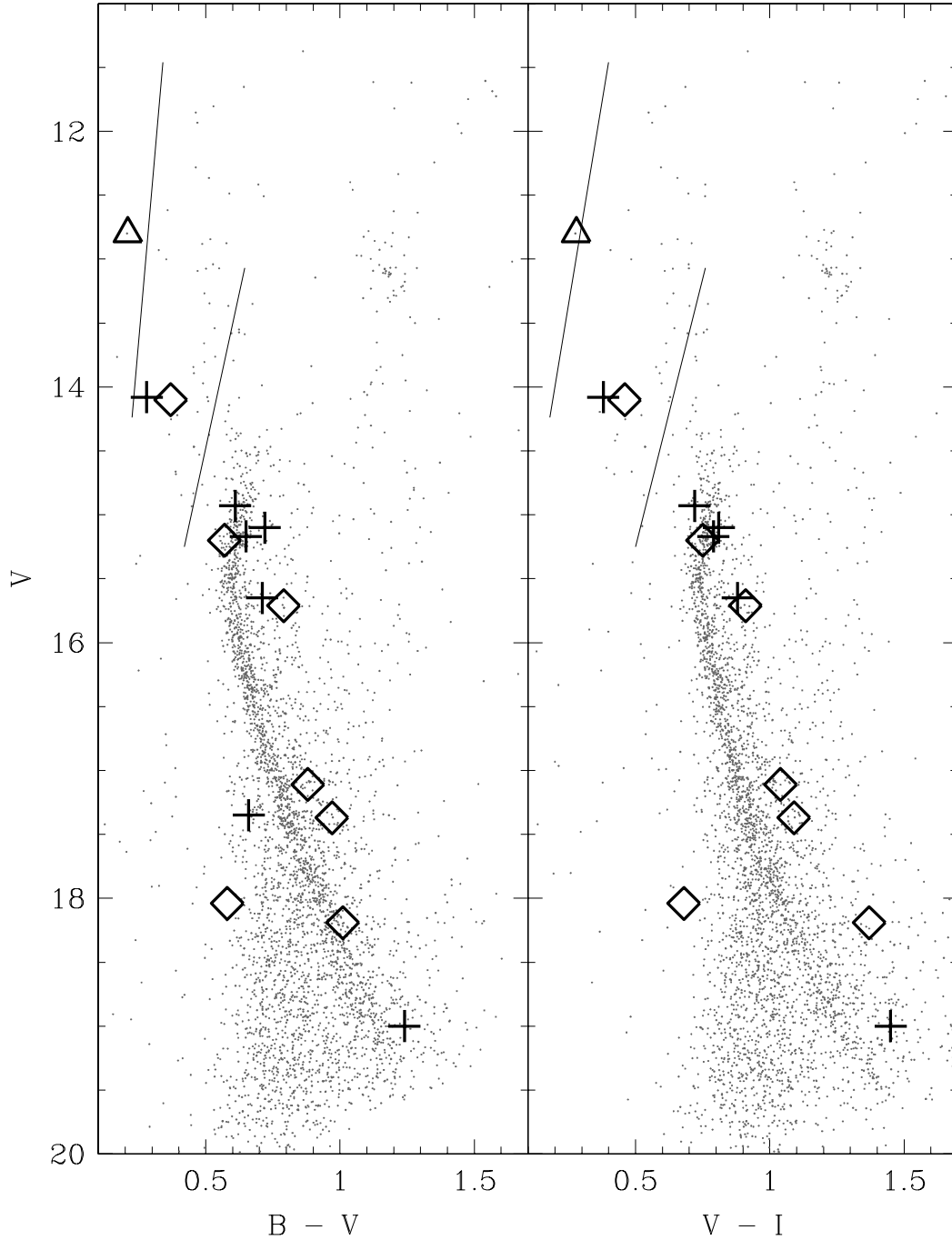


Fig. 4.— Color-magnitude diagram for NGC 6819 with variables identified. Detached eclipsing binaries are shown with crosses, contact and near contact binaries are shown with diamonds, and pulsating variables are shown with triangles. Solid lines are the theoretical instability strip from Pamyatnykh (2000).

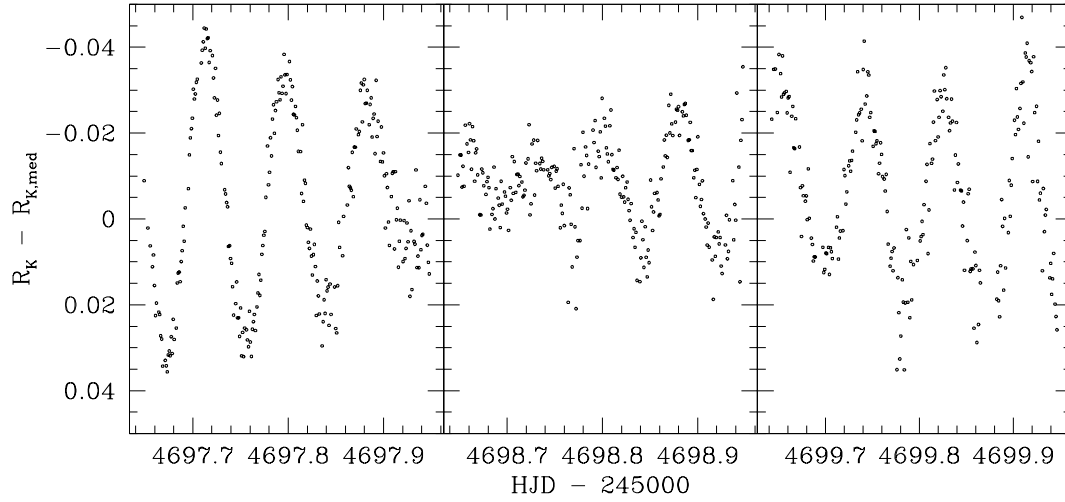


Fig. 5.— Selected nightly light curves for the  $\delta$  Scu variable A20pe. In this and all subsequent figures, the median for our observations in each filter band has been subtracted.

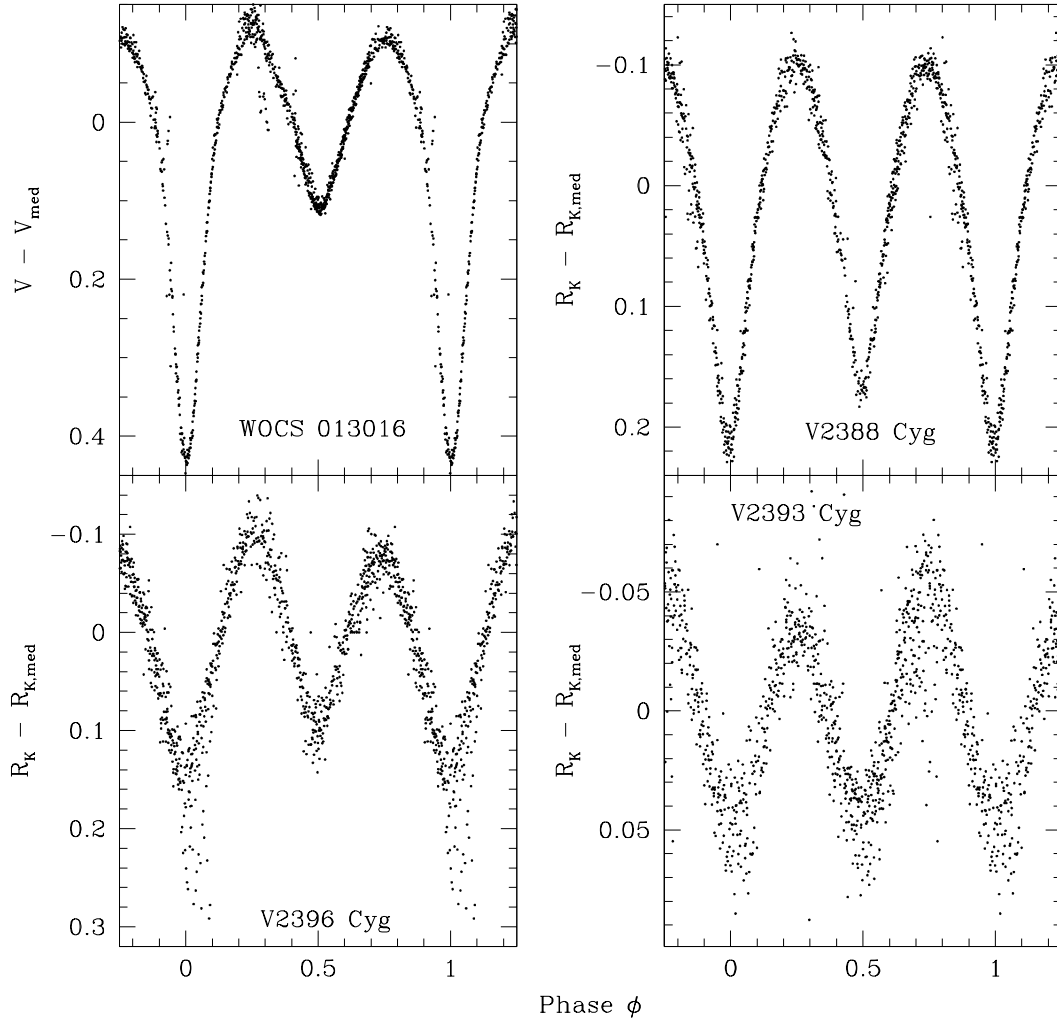


Fig. 6.— Phased light curves for contact and near-contact binaries.



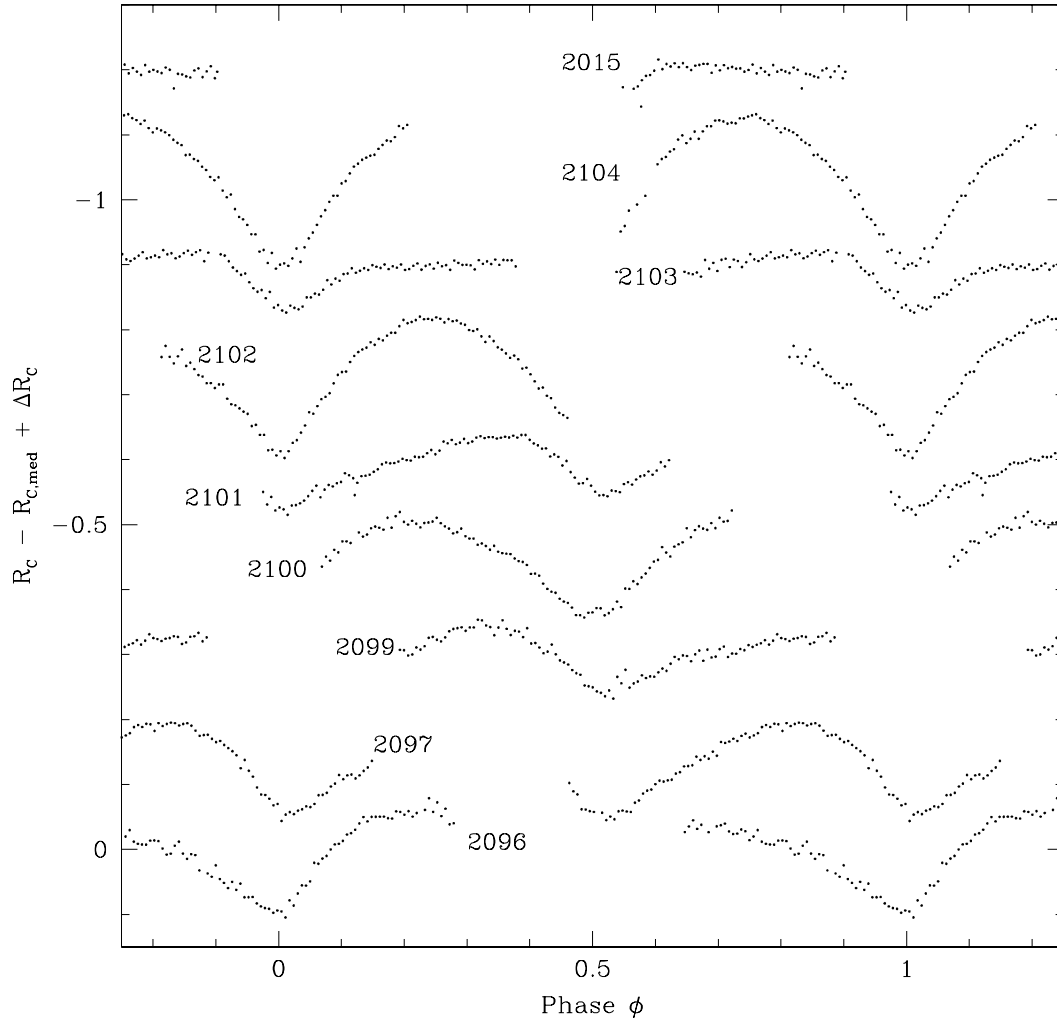


Fig. 7.— Phased light curves from individual nights of observations in  $R_C$ . Numerical labels corresponds to the heliocentric Julian date at the start of observations minus 2450000. Each night was shifted brightward in the plot by 0.15 mag from the previous night plotted.

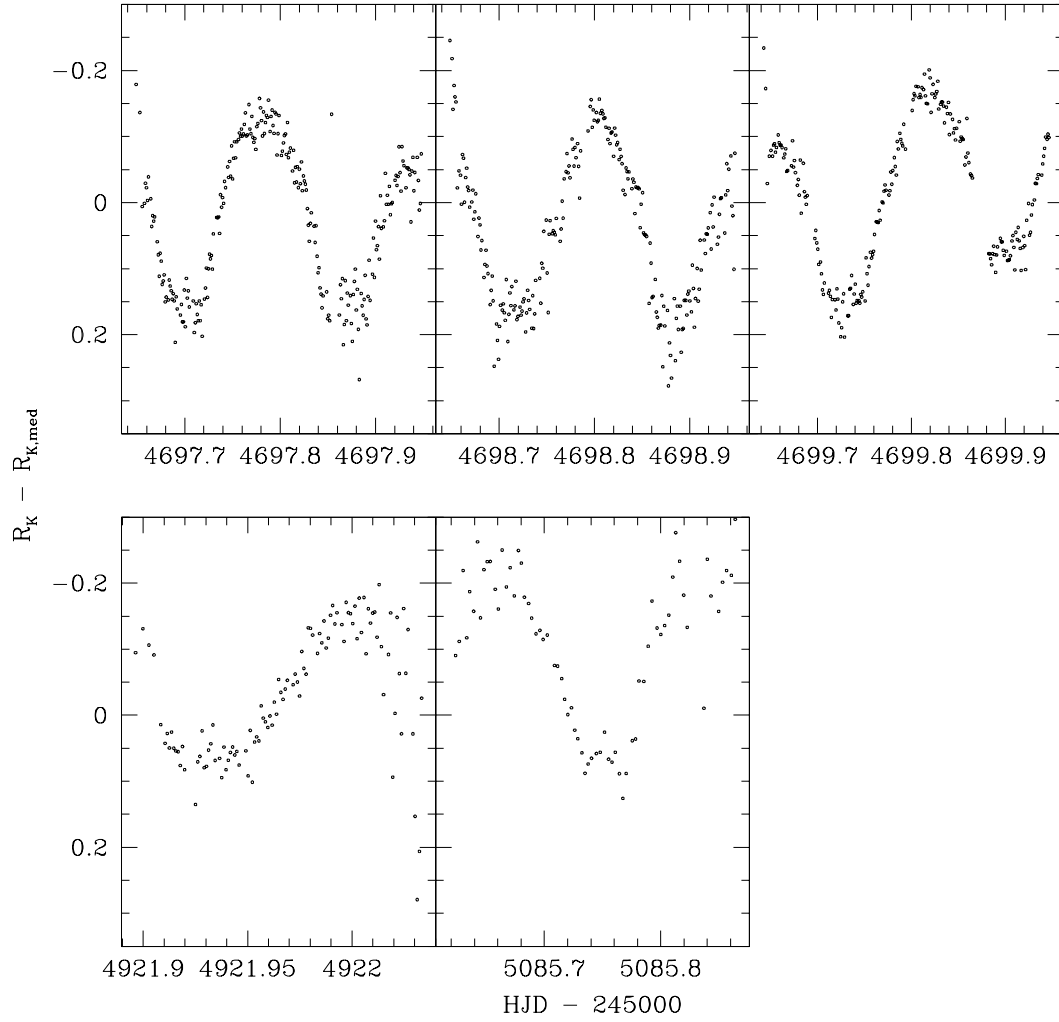


Fig. 8.— Nightly light curves in  $R_K$  for V2389 Cyg.

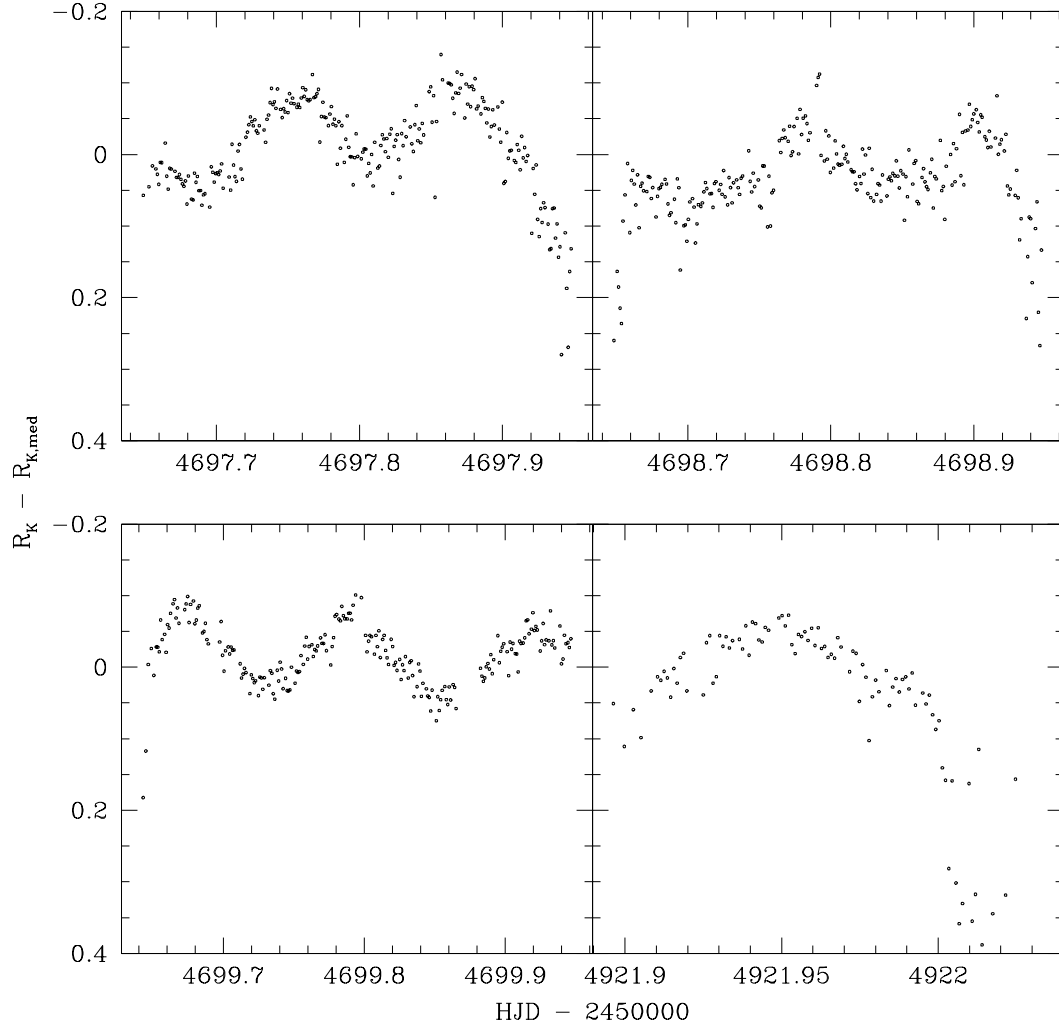


Fig. 9.— Selected nightly light curves in  $R_K$  for V2394 Cyg.

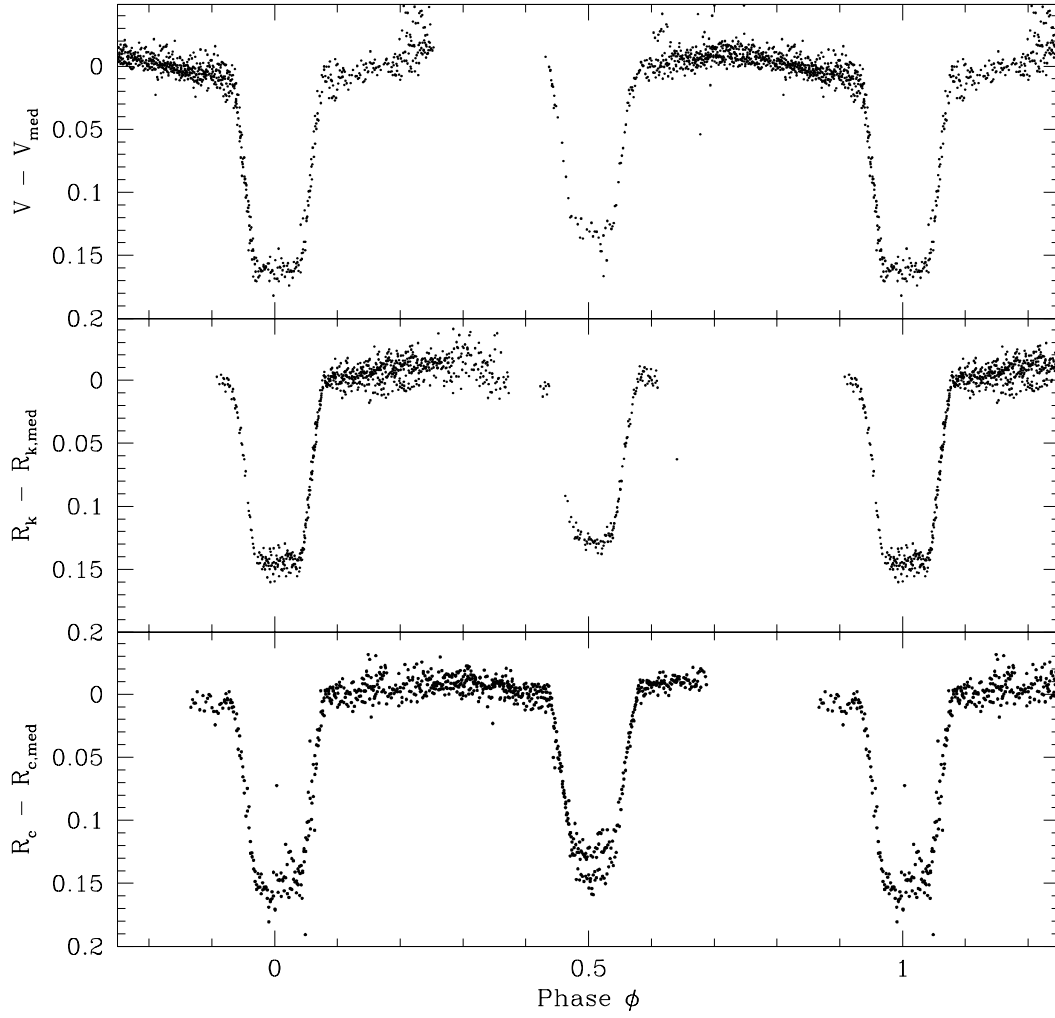


Fig. 10.— Phased light curves for A494.

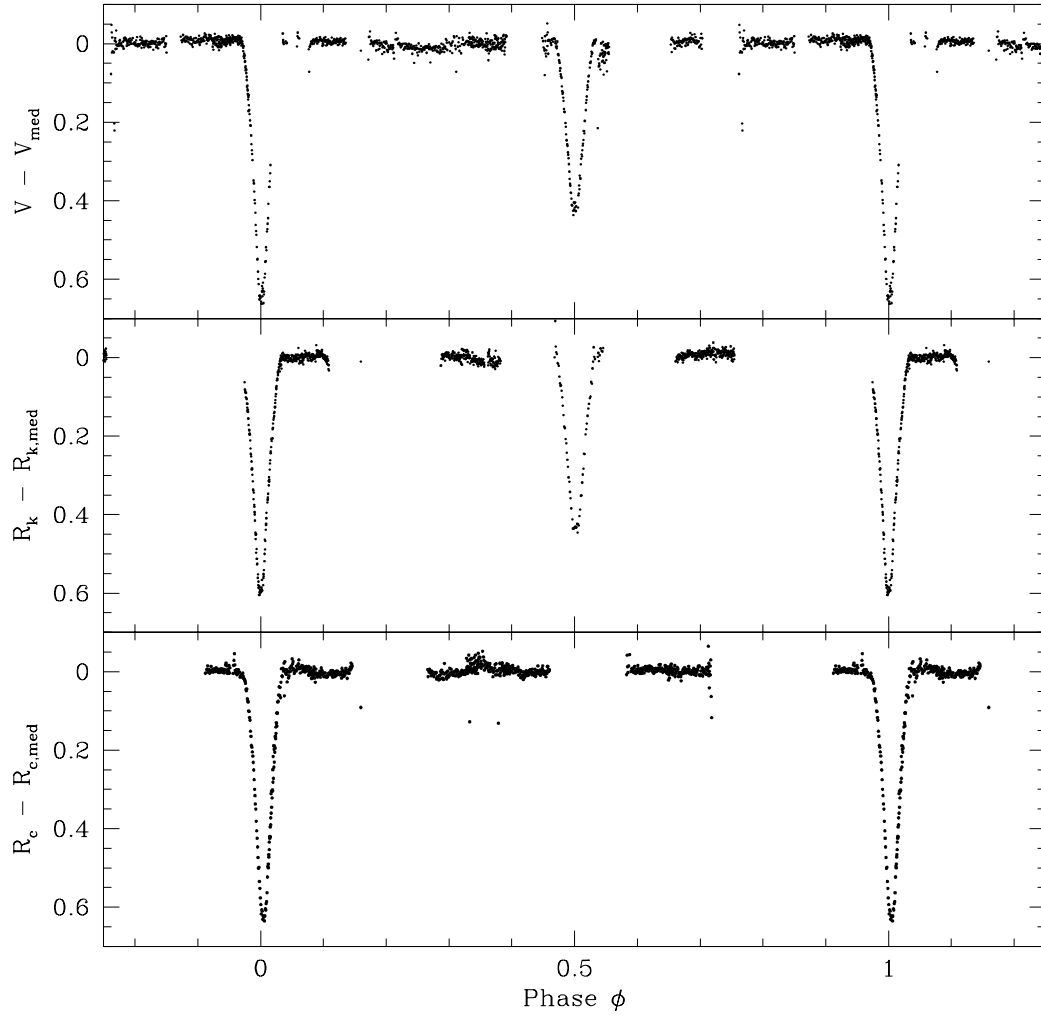


Fig. 11.— Phased light curves for A259.

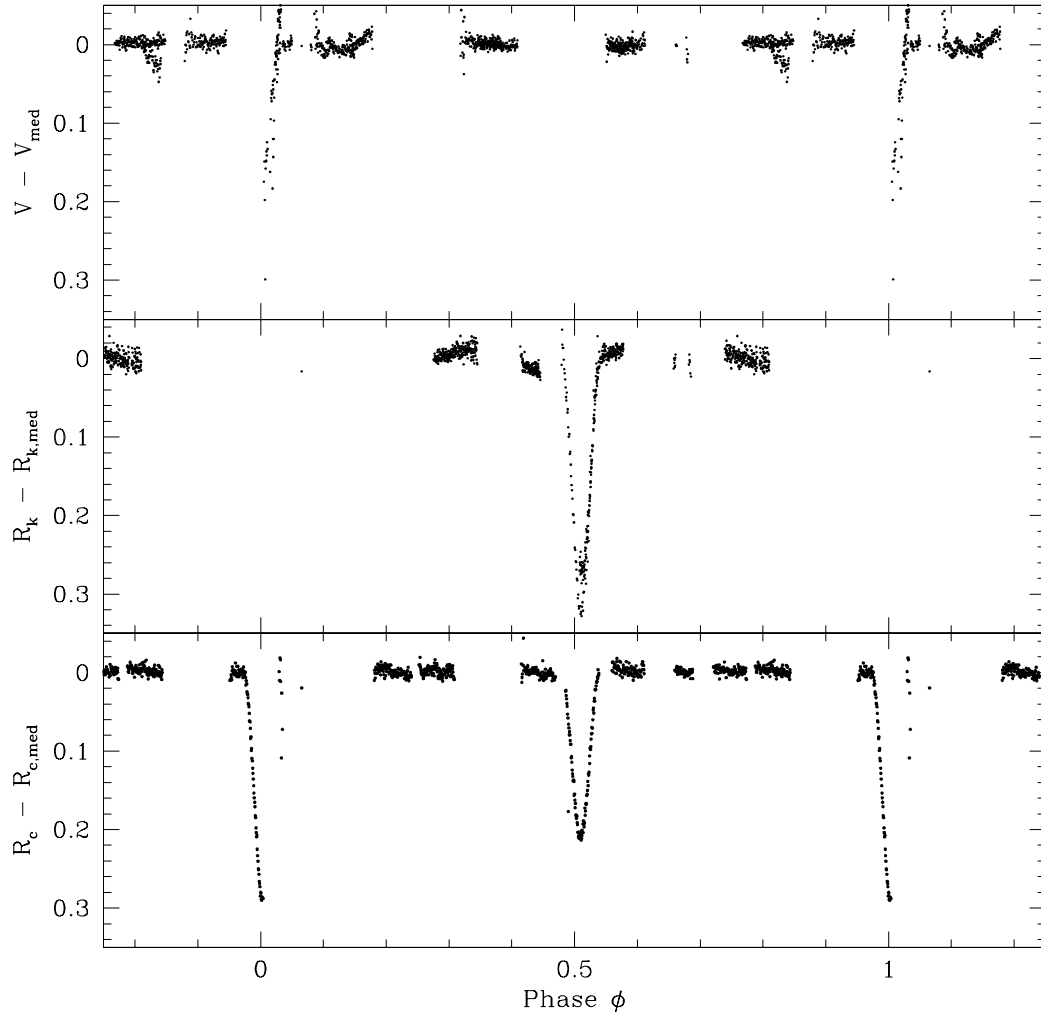


Fig. 12.— Phased light curves for A536. The employed period comes from radial velocity observations (A. Geller & R. Mathieu, private communication).

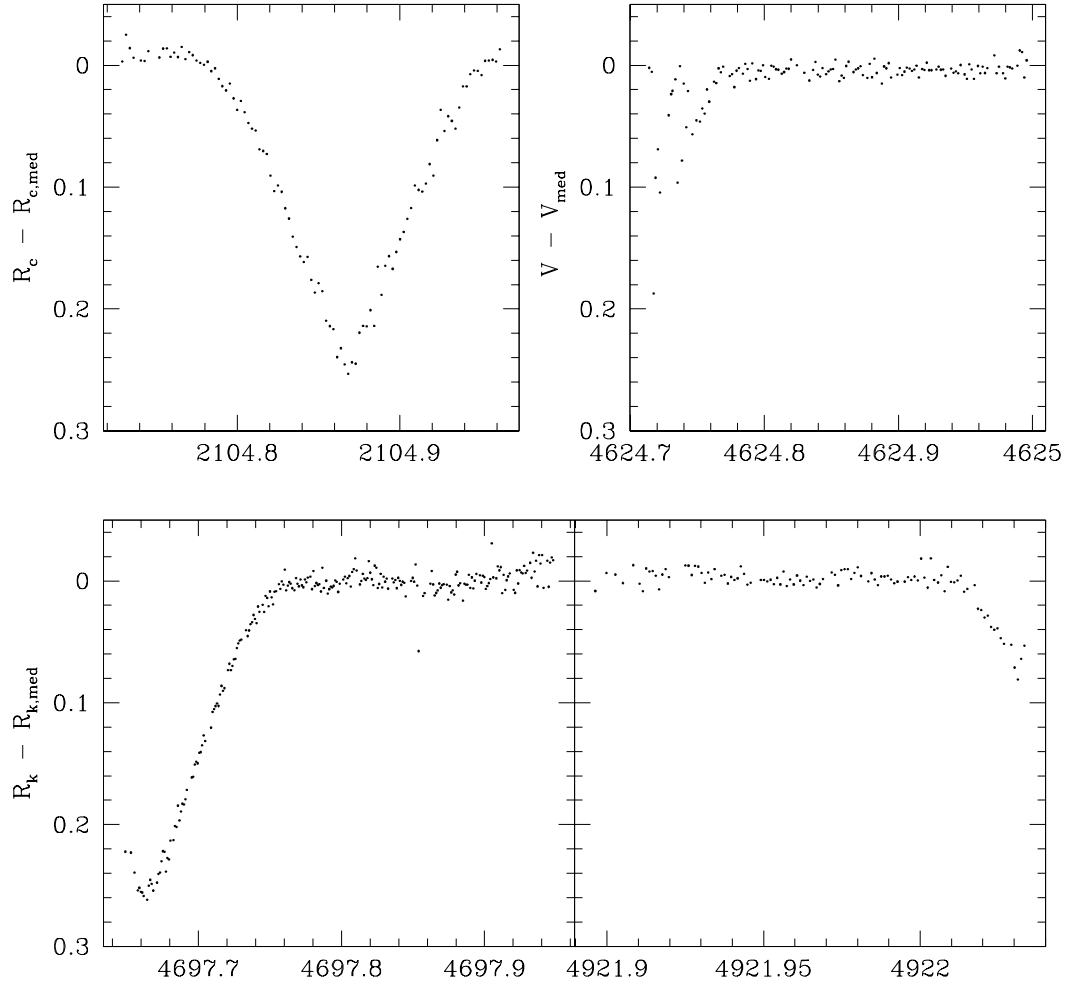


Fig. 13.— Light curves for nights with detected eclipses for A665.

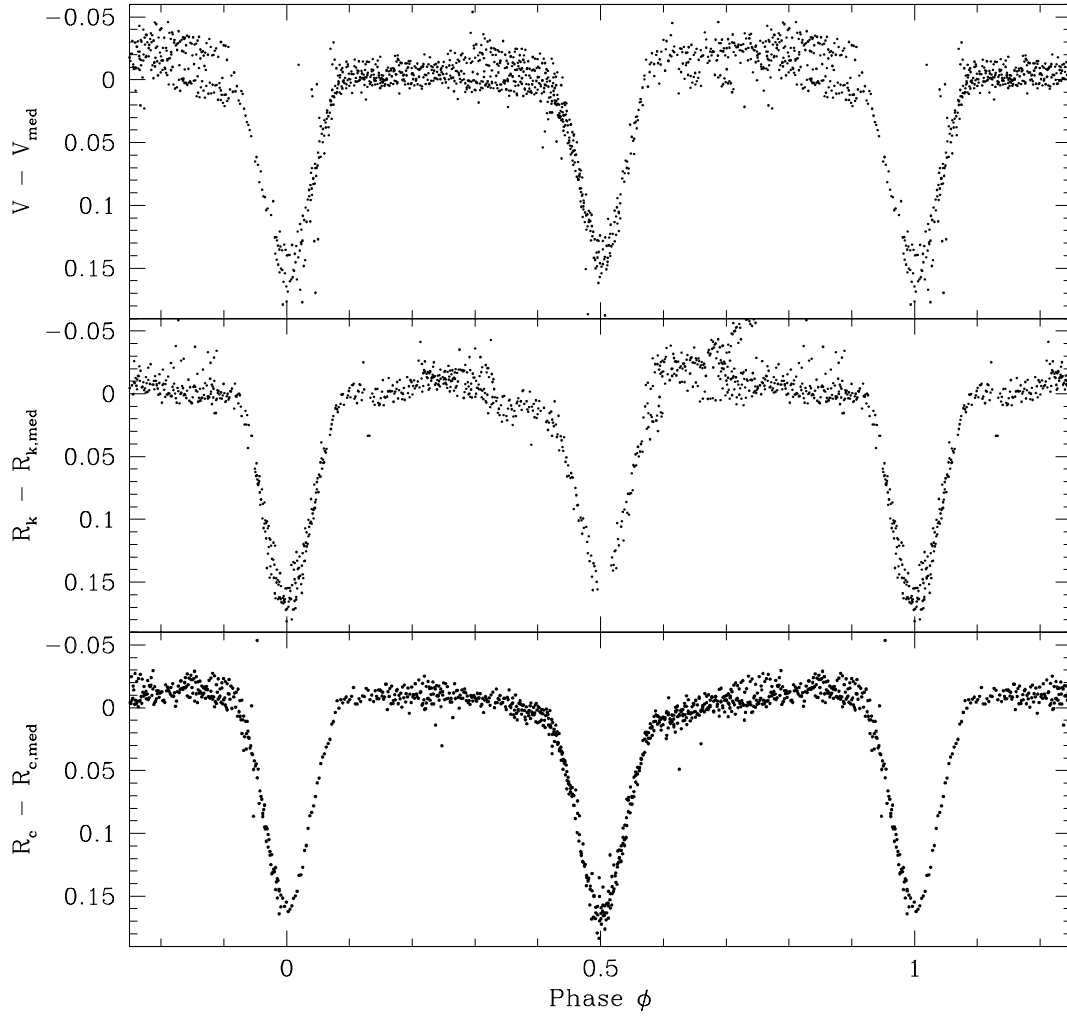


Fig. 14.— Phased light curves for A824.



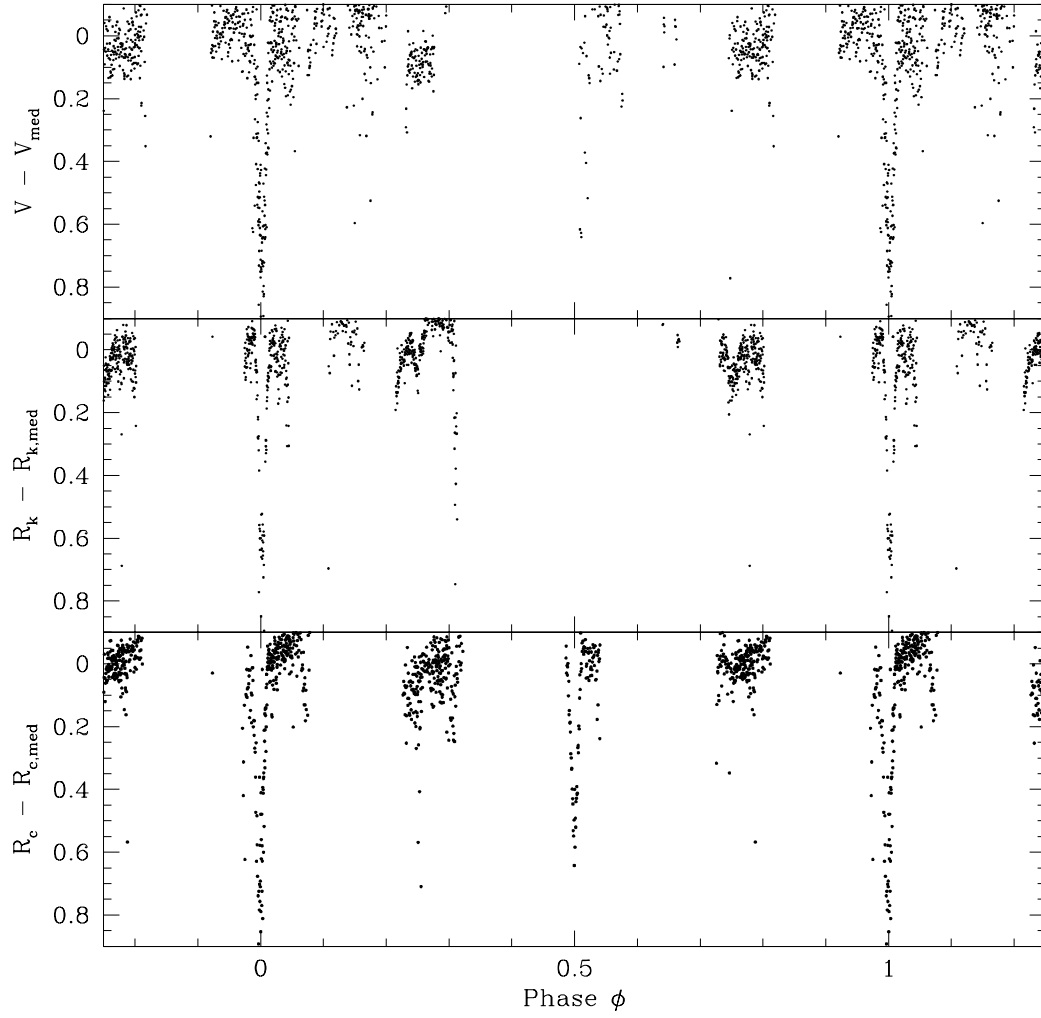


Fig. 15.— Phased light curves for ID 1602.